

# Integrated Geoelectrical Resistivity Method for Environmental Assessment of Landfill Leachate Pollution and Aquifer Vulnerability Studies

Stanley U. Eze<sup>1</sup>, Omafume M. Orji<sup>2</sup>, Abriku E. Onoriode<sup>3</sup>, Saleh A. Saleh<sup>2</sup>, Macpaul O. Abolarin<sup>2</sup>

<sup>1</sup>Department of Earth Sciences, Federal University of Petroleum Resources, Effurun, Nigeria

<sup>2</sup>Department of Petroleum Engineering and Geosciences, Petroleum Training Institute, Effurun, Nigeria

<sup>3</sup>Department of Physics, Delta State University, Abraka, Nigeria

Email: uchechukwueze2014@gmail.com, orji\_om@pti.edu.ng

**How to cite this paper:** Eze, S. U., Orji, O. M., Onoriode, A. E., Saleh, S. A., & Abolarin, M. O. (2022). Integrated Geoelectrical Resistivity Method for Environmental Assessment of Landfill Leachate Pollution and Aquifer Vulnerability Studies. *Journal of Geoscience and Environment Protection*, 10, 1-26.

<https://doi.org/10.4236/gep.2022.109001>

**Received:** June 14, 2022

**Accepted:** September 3, 2022

**Published:** September 6, 2022

Copyright © 2022 by author(s) and Scientific Research Publishing Inc.

This work is licensed under the Creative Commons Attribution-NonCommercial International License (CC BY-NC 4.0).

<http://creativecommons.org/licenses/by-nc/4.0/>



Open Access

## Abstract

Leachate plumes from landfills are a major source of pollution in Nigeria, especially in urban areas. Assessing leachate contamination in the subsoil is considered a complex process that needs detailed field measurement to accurately define the extent of contamination. To ascertain the extent of pollution of the subsoil and groundwater sources which were reportedly contaminated by leachate plumes from an old dumpsite located in Osubi town, an integrated geoelectrical method involving 1-D vertical electrical sounding (VES) and 2-D, 3-D ERT techniques were employed. Orthogonal set of 2-D apparent resistivity data was collected in a 100 × 50 m<sup>2</sup> rectangular grid around the dumpsite, using the Wenner array. Two years later, three (3) 2-D resistivity imaging profiles were also recorded in time-lapse mode at the dumpsite to monitor the possible effects of attenuation on the leachate over time. Ten (10) VES data were also acquired and used along with the 2-D imaging data. 2-D apparent resistivity data were inverted with Dipprowin software program. The orthogonal set of 2-D lines of apparent resistivity was merged into 3-D data and inverted with RES3DINV program to create a 3-D subsurface resistivity model. Geological models observed from 2-D and 3-D resistivity inversion revealed low resistivity values in the order  $\rho < 100 \Omega \cdot m$  which is indicative of leachate plumes in the saturation zone (pore water). The 2-D resistivity-depth sections imaged low resistivity leachate plumes at the near surface (<5 m) to a depth of 25.0 m, while 3-D inversion depth slices imaged leachate contaminant within the first, second and third layers at depth ranging from 0.00 - 2.50 m, 2.50 - 5.38 m and 5.38 - 8.68 m respectively. Thus, leachate contamination clearly increased with depth beyond the depth of first and second aquifers in the area which implies that available groundwater for domestic use is already contaminated with leachate from the dumpsite. Leachate con-

---

taminant-depth map estimated for the second geoelectric layers for VES 2, 3, 4, 7, 8, 9, and 10 shows that the second layer has been invaded completely by leachate contamination up to 6.5 m depth. 2-D apparent resistivity data acquired two years after show lower resistivity anomalies of the leachate plume caused by time-lapse attenuation effect on the observed resistivity of the leachate. This indicates that the leachate plume has become more conductive and toxic to the environment. The Longitudinal conductance map of the area shows that the aquifer protective capacity of this area is weak (0.1 - 0.19 Mho) thus, aquifers in the area are prone to pollution from the dumpsite. The three techniques used in this study (2-D, 3-D ERT and 1-D VES) fitly provided crucial information on the degree of contamination caused by the landfill leachate plume. Therefore, it is advisable to implement an environmental remediation and leachate management program.

### Keywords

Leachate Contamination, Groundwater Pollution, 2D and 3D Electrical Resistivity Tomography (ERT), Aquifer Vulnerability, Environmental Assessment

---

## 1. Introduction

Groundwater pollution is in particular, among the most severe environmental problems especially around and within areas with history of industrial-based activities. Contamination sources could be point or areal sourced contamination. Point-source contaminants include landfills, industrial disposed waste, random runoff, petrol tanks, and more. Areal contaminants are, for example, chemicals used in farming like fertilizers/pesticides. Under point source pollutants, landfill that has different types of solid-waste is common, and could possibly generate leachate plume, which can pollute both surface and groundwater sources (Kjeldsen & Christophersen, 2001; Cozzarelli et al., 2011; Carpenter et al., 2012). Leachate is a term widely used in environmental science and has the distinct meaning of a liquid that dissolves or accompanies a pollutant released into the environment. This can affect the functioning of ecosystems, as leachates can contain both old and new pollutants (Lapworth et al., 2012; Chung et al., 2018). Over time, landfill waste will decompose and dissolve, producing leachate containing inorganic and organic components as water permeates from the landfill.

In many cases, old landfills have no leachate collection or liner placed under the landfill. This could lead to leachate contaminating groundwater down-gradient from the landfill. Leachate plume movement (see **Figure 1**) can contaminate surface-water and aquifers for decades posing serious long-term environmental and health risks (Bjerg et al., 1999, 2014). This plume contains carcinogenic substances in the form of dissolved heavy metals such as lead, arsenic, mercury, cadmium and chromium, and less harmful ions such as sodium

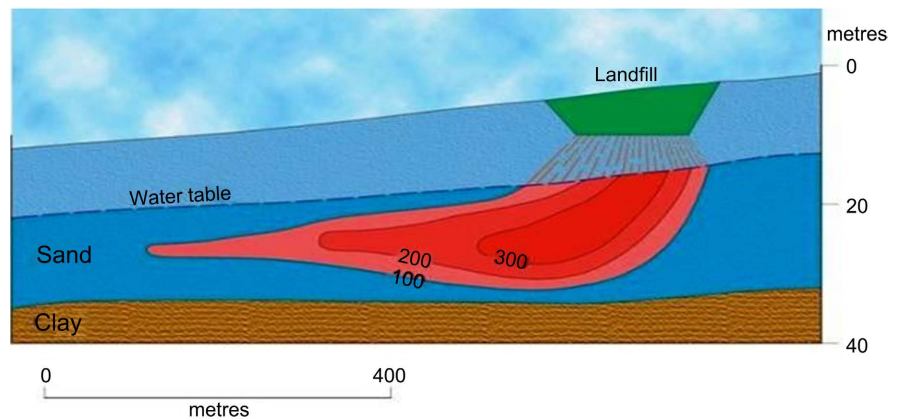


**Figure 1.** Conceptual diagram of a groundwater contamination plume from a landfill (contours represents a generic-contaminant concentration (adapted from Christensen et al., 2001).

and calcium. Understanding the interaction between the surrounding aquifer and contaminant plume is becoming increasingly important in assessing these risks. Therefore, the main purpose of landfill surveys is to map and characterize contaminant plumes.

The most commonly used techniques for this purpose are hydro-geological and geological description of aquifer features using borehole information and chemical analysis of water/soil specimens. However, these procedures give insufficient spatial information, which could result to deficient investigation of the site and insufficient remediation designs. Geophysical surveys can provide a wide range of adjacent coverage along with better resolution information and reduces the possible gap in spatial information. Leachate is a complex mixture of organic carbon, primarily in the form of “fulvic acid,” which makes the contaminated groundwater conductive. A rise in conductivity of contaminated groundwater could be ascertained from the surface using the method of non-invasive geo-electrical resistivity. This provides a relatively cheaper way to map pollution faster without monitoring of wells. A good review of the myriad references which use this technique in tracking pollution in groundwater was published in (Meju, 2000; Zonge et al., 2005; Carpenter et al., 2012; Ayolabi et al., 2013; Ofo-mola, 2015; Ofo-mola et al., 2016).

Electrical conductivity and resistivity are reciprocals of each other.

Generally,  $\sigma$  represents electrical conductivity its unit is Siemen per meter (S/m), while the symbol  $\rho$  represents electrical-resistivity unit is the Ohm-meter ( $\Omega$ -m).

The relation between the two is:

$$\sigma = 1/\rho \quad (1)$$

$$\rho = 1/\sigma \quad (2)$$

Electrical-resistivity tomography is a technique for geophysical imaging commonly employed in pollution research, archaeological mapping as well as in civil

engineering. Two-dimensional (2-D) geoelectrical resistivity tomography is already used successfully by numerous scholars in detecting contaminant plumes (Goes & Meekes, 2004; Ayolabi et al., 2013). In 2-D model interpretation, it is noticed that resistivity of the subsurface change in vertical and lateral dimensions along the survey lines (Loke, 2001). But, geological features and subsurface spatial distributions of pollutants usually encountered in hydro-geological and environmental assessments are three-dimensional (3-D) in geometry. Thus, images obtained using 2-D electrical resistivity surveys could contain misleading features because of 3D effects that results in inaccurate interpretation of this anomaly with respect to position (Loke, 2000). This is a major limitation of the 2-D resistivity model. As a result, the 3-D ERT method offers better resolution and effectiveness than the 2-D resistivity method in depicting of contaminated zones and layers. The primary purpose of this study is to map leachate plumes generated from an open landfill, to assess the extent of environmental and groundwater pollution from the landfill, possible dampening effects of leachate resistivity over time, and assess the vulnerability of the aquifers in the dumpsite. This requires the integration of geoelectric resistivity methods with 1-D, 2-D, and 3-D techniques.

### 1.1. Background of the Study Area

The research landfill is an open dumping system (Figure 2) located in the city of Osubi. Osubi is a town sited in Okpe local government area of Delta State (Figure 3) and is located at latitude  $5^{\circ}33'0''\text{N}$  and longitude  $5^{\circ}47'0''\text{E}$  in the geographical location. Osubi is rapidly becoming a vibrant modern community with faster expansion and architectural projects for modern living being implemented in the area. Here you will find the world-famous Nigeria-Petroleum Training Institute (PTI). Warri airport is located in this area and there is massive infrastructural development in the area. These have resulted to the massive migration of population to this area accompanied by massive and indiscriminate dumping of domestic and industrial waste, which directly threatens the environment, especially the quality of surface water and groundwater.



(a)



(b)

**Figure 2.** Physical condition of the dumpsite as at the time of this survey in Osubi, Delta State, Southern, Nigeria.

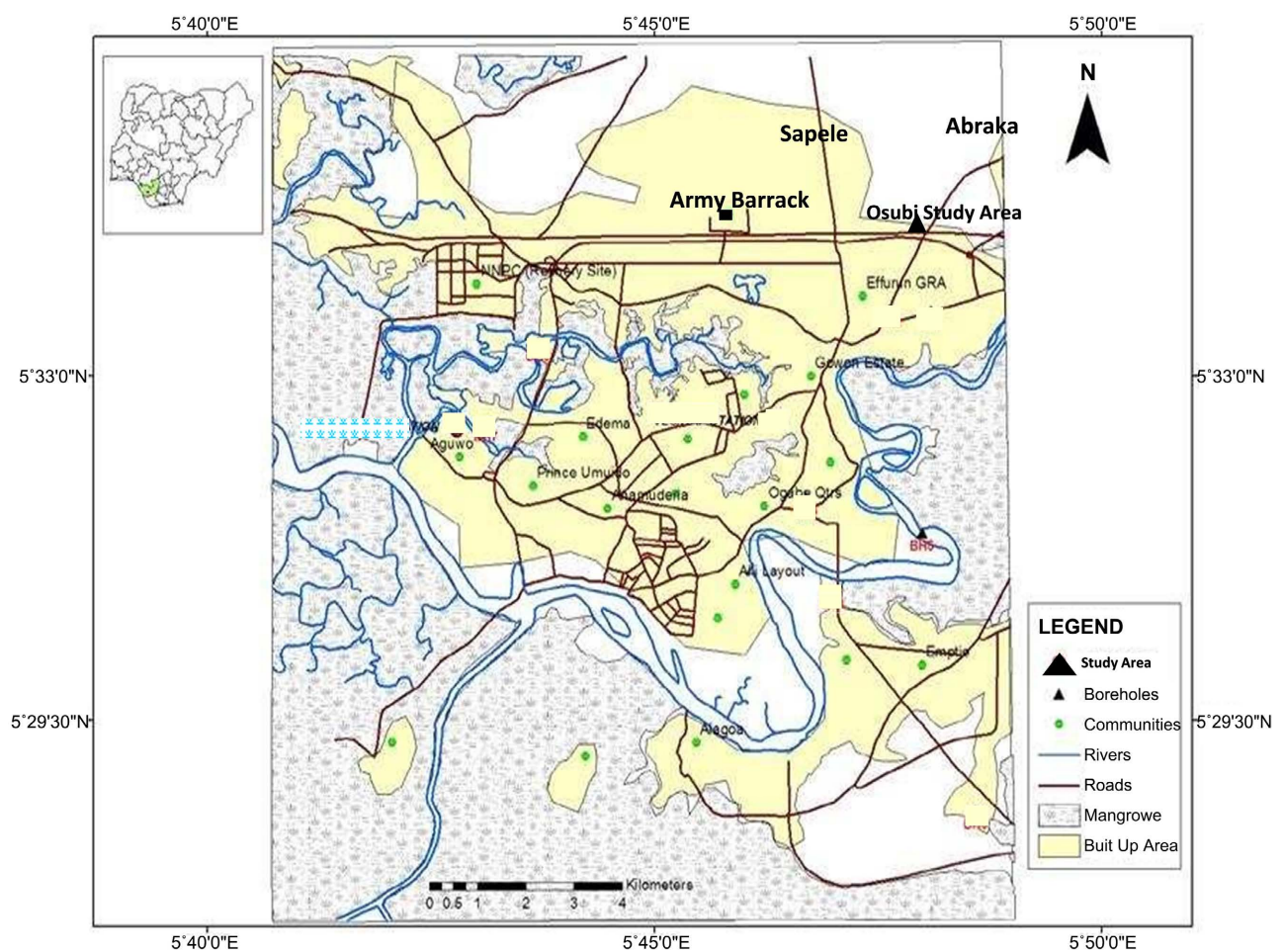


**Figure 3.** Map of Warri Delta State, showing the study area, communities, built up areas between: 1986-2002. (Map drawn by Professor F.O. Odermeh, and modified from *Ofofola, 2015*).

The research landfill is located along the Eku-Warri highway across from the Osubi Slaughter Market, a few miles from the new facility of PTI in Osubi, Delta State. It is sited around the geographical coordinates of “latitude 5° 39.638’N and longitude 5° 49.000’E” (**Figure 3**) with an area of 100 × 100 m<sup>2</sup>.

## 1.2. Geology of the Study Area and Hydrogeology

The geology of the study area Osubi-near Warri is located in the Niger Delta, and the geology of this area has been studied by a number of researchers (Aseez, 1989, Reyment, 1965, along with Short & Stauble, 1967). The Osubi region is characterized by almost flat topography, with a very gentle slope towards the sea (Akpokodje & Etu Efeotor, 1987), beneath which includes Quaternary, Sombriero Deltaic plain sand (Figure 4). According to Wigwe (1975), Olobaniyi & Owoyemi (2006), this formation comprises of fine to medium loose grain sand and feldspar of about 30% to 40% by weight. The Niger Delta is composed of three stratigraphic formations overlain with Quaternary-deposits (Short & Stauble, 1967). Stratigraphic formations comprises of Benin, Agbada and Akata formations. Typical sections of these formations are summarized in Short & Stauble (1967) and other reports such as Doust & Omatsola (1990), Kulke (1995). The Akata Formation comprises mostly of marine shale and sand layer, and its subsoil consists of dark gray sand and shale. The thickness of this Formation is estimated to be more than 7000 m (Doust & Omatsola, 1990). The upper Agbada Formation is a series of sandstone and shale-deposits (Merki, 1970). It consists

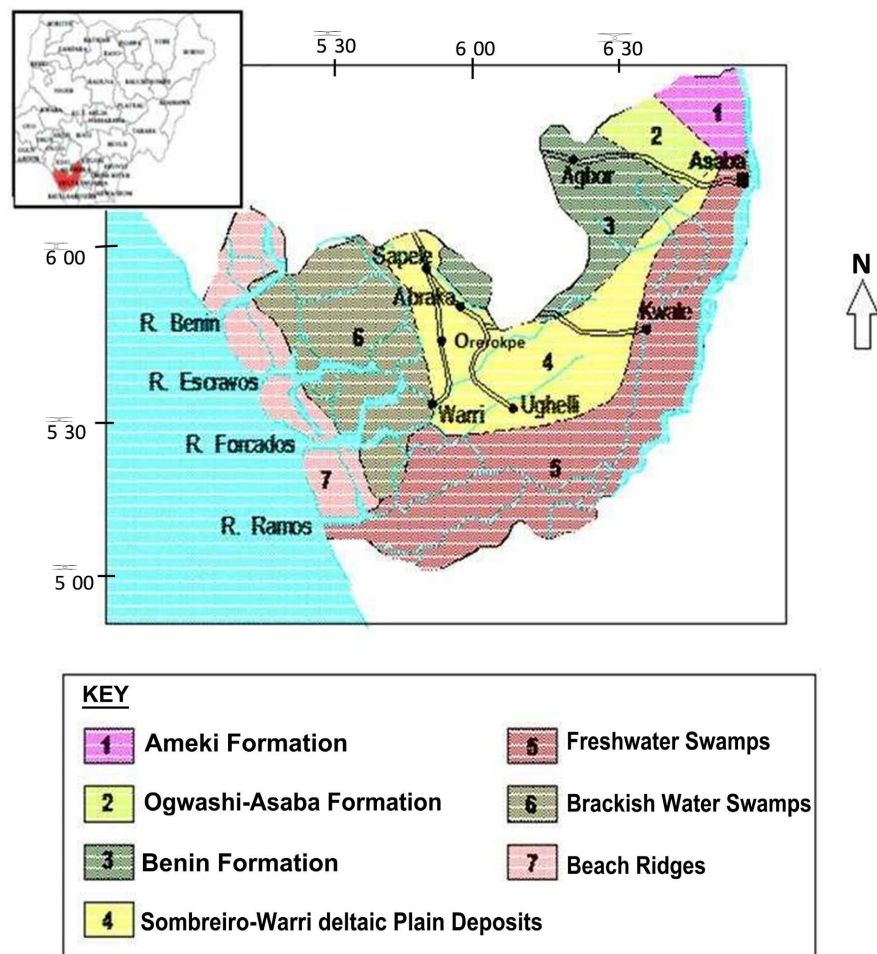


Figure 4. Geological Map of Delta State (modified from Akpoborie et al., 2011).

of the upper part mainly sand with a small number of shale and lower end containing shale. The thickness is over 3700 m. The upper layer of Benin is covered in many places by thin laterite layers of varying thickness, but is much more exposed near the coast. The main aquifer units in this area are located in the upper delta lithofacies (Akuijeze & Ohaji, 1989). The water-table in the area (the first existence of groundwater below the subsurface) is estimated to occur between 4 to 5 m beneath (Uchegbulam & Ayolabi, 2014).

### 1.3. Electrical Resistivity Anomalies in Relation with Leachate Plume Contamination and Attenuation

Geophysical techniques are widely used to study surface and underground pollution caused by various types of pollutants. Leachate are liquids formed from decomposed waste and they have appreciable electrical conductivity because of dissolved salts. Thus, resistivity of leachate is lower compared to groundwater. Leachates have high concentrations of ions and therefore lead to low resistivity in rock formations containing them (Cristina et al., 2012) thus, making electrical resistivity technique useful in mapping and locating levels of leachate contamination within landfills (Bernstone & Dahlin, 1999). Studies on landfill geo-electrical resistivity have been conducted by numerous researchers on soil/groundwater contamination (Jhamnani & Singh, 2009; Abdullahi et al., 2011; Jegede et al., 2012; Ayolabi et al., 2013; Ganiyu et al., 2015).

Pollutants released into the environment hardly remain stationary at the released point rather they are easily conveyed via porous channels by four main processes and mechanisms, namely adsorption, convection, diffusion, and mechanical dispersion (Marylyn, 1990; Ganiyu et al., 2015). Adsorption affects the fate of chemicals (contaminants) in the soil and considered as the most essential transport process that determines their distribution in soil and water-based environments (Lyngkilde & Christensen, 1992; Kah & Brown, 2007). Pollution of groundwater take place mostly because of river water infiltration and percolation of pollutants via the soil at landfills (Abdullahi et al., 2011).

Leachate pollution of the environment and water sources is a complex phenomenon because there are some processes of attenuation that control contaminants in aquifers affected by leachate. Attenuation here refers to dilution, absorption, ion exchange, precipitation, oxidation/reduction reaction, and decomposition processes (Giang et al., 2018). Not minding the fact that natural attenuation and weathering processes underground helps to minimize possible impacts of leachates, their essence depends on climatic and geological features and also on the quality of involved leachates.

Geophysical methods are useful tools for assessing and delineating pollution plumes, as well as their changes over time, allowing cost-effective monitoring. In this study, the source of pollution studied is an old municipal waste landfill system. Therefore, attempt was made to separate these contaminated layers considering the low apparent resistivity anomaly observed, and then an assessment of possible attenuation impact on apparent resistivity values of the leachate was

conducted using apparent resistivity data acquired two (2) years (in time-lapse mode) after the completion of the first geophysical survey in the dumpsite.

## 2. Methods

### 2.1. Geophysical Investigation

#### 2.1.1. 1-D Vertical Electrical Sounding (VES) and 2-D Electrical Resistivity Tomography (ERT)

First, confirm that In this study, Orthogonal series of 2-D ERT data consisting of six (6) parallel and six (6) vertical traverses were acquired in the studied dumpsite using PASI-16GL imaging system, using the conventional Wenner electrode arrangement known as Wenner alpha, in a  $100 \times 50 \text{ m}^2$  rectangular grid, forming traverses  $LY_1 - LY_6$  (called 2-D in-line traverses) in Y-direction and  $LX_1 - LX_6$  known as 2-D cross-line traverses in X-direction. Inter-traverse spacing in both cross-line and in-line directions are 20 m and 10 m, respectively (Figure 5). The 2-D Wenner technique was used because of its remarkable sensitivity to depth and the Wenner array is outstanding in determining vertical alterations in subsurface resistivity i.e horizontal structures (Loke, 2010). Ten (10) vertical electrical soundings were also obtained from the studied dumpsite using the Schlumberger array to provide 1-D layering information and to support the 2-D imaging data. The purpose of the VES survey is to appraise the aquifer vulnerability of the area by computing its overburden protective capacity to assess the condition of shallow aquifers and also to ascertain trends in leachate contamination with respect to depth. This will guide future groundwater production practices in the area.

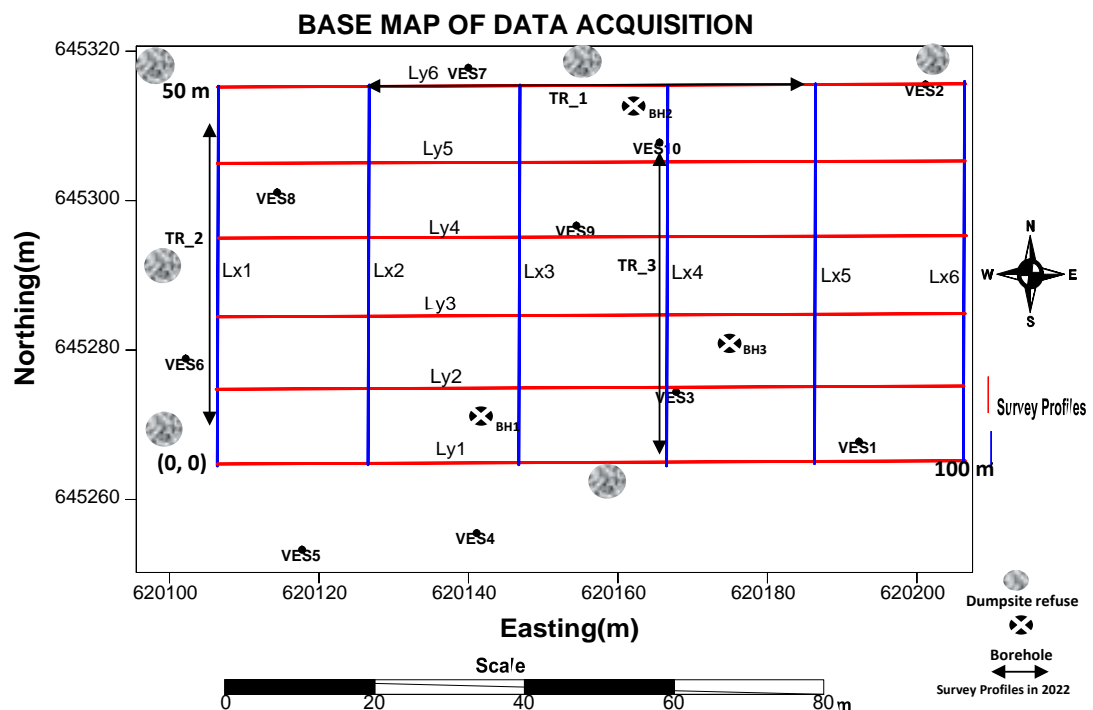


**Figure 5.** Base map of data acquisition, showing the initial 2-D Grid lines, recent survey profiles, VES stations occupied and borehole locations in the study dumpsite, Osubi, Delta State, Southern Nigeria.



In this study, an attempt was made to examine the possible attenuation effect that the leachate contaminants might undergo over time. To this end, after a period of 22 months (February 2020-January 2022), another 2-D resistivity imaging survey was conducted on the dumpsite. The first geophysical survey on the dumpsite was completed on February 8, 2020, and was a 2-D grid survey. The second geophysical survey was conducted on January 13, 2022 (a time-lapse interval of almost 2 years) immediately after a heavy rainfall. However, due to the physical constraints at the dumpsite in 2022 (swamp water, excess debris and vegetation etc.), the second geophysical survey was conducted in profiles rather than a grid. Three 2D traverse lines labeled TR\_1, TR\_2, and TR\_3 as shown in the base map (**Figure 5**) were acquired at the dumpsite along the 2D traverses Ly<sub>6</sub>, Lx<sub>1</sub>, and Lx<sub>4</sub> of the first survey (**Figure 5**). The acquisition was designed so that the traverses (TR\_1, TR\_2, and TR\_3) closely matched the electrode positions of the 2D traverse lines occupied in the first geophysical study. This was done to monitor the possible time-lapse attenuation effect of the resistivity of the observed leachate contaminants over time.

### **2.1.2. 3-D Electrical Resistivity Tomography (ERT)**

To ensure better study coverage on the dumpsite and to ensure correct interpretation, 3-D resistivity interpretation that gives the most suitable and correct results (Loke, 2000) was implemented based on the orthogonal 2-D apparent resistivity data. Presently, the cost of carrying out a 3-D resistivity survey is high compared to 2-D surveys (Loke, 2000). However, current advances in fast forward modeling software's (Loke, 1994; AGI, 2003) has helped for accurate simulation of bulk volume of 2-D data in both orthogonal and parallel profiles into 3-D dataset within a notable time. This is a more practical and realistic means for generating 3-D geoelectrical resistivity data in the field.

## **2.2. Determination of Hydraulic Head Distribution and Groundwater Flow Direction**

Three (3) boreholes found at the dumpsite at different locations were marked as BH1, BH2 and BH3. The boreholes were positioned in a triangular fashion (**Figure 5**), therefore this enabled the determination of the flow direction of groundwater in the dumpsite by determining the steady state hydraulic head distribution. The hydraulic head was determined as the difference between the surface elevation of each well and the static water level. The surface elevations are 18 m, 10 m and 12 m while static water levels were 3.50 m, 6.50 m and 4.50 m in BH1, BH2 and BH3 respectively. The hydraulic head was higher at BH<sub>1</sub> (14.5 m), lowest at BH<sub>2</sub> (3.5 m) and moderate at BH<sub>3</sub> (7.5 m). Groundwater flows from regions of higher hydraulic gradients to regions with lower hydraulic gradients. In between the wells in the dumpsite, the data points are sparse and needs to be interpolated using a computer software to interpolate sparse data points into a regular grid. SURFER-13 gridding and contouring software program (2002), using the triangulation with linear interpolation method was used to interpolate

the points and the interpolated values were contoured.

### 2.3. Geophysical Data Processing and Inversion

VES data was processed using the manual-curve matching process to obtain curves of resistivity models, which were also curve matched with the auxiliary and master curves and layer variables obtained was entered into Win-Resist computer platform (Vander Velpen, 2004) and interpreted quantitatively to obtain the one-dimensional resistivity model parameters which are thickness and layer resistivity from which leachate contaminated geoelectric layers (with relatively low apparent resistivity values) were inferred.

Quantitative interpretation of VES data generates the layer parameters (thickness and layer resistivity) which are otherwise known as the first-order geoelectric parameters (the layer thickness  $h_i$  and the layer resistivity  $\rho_i$  for the  $i^{\text{th}}$  layer ( $i = 1$  for the topmost layer). These first-order geoelectric parameters were utilized to derive longitudinal unit conductance ( $S_i$ ) of all the geoelectric layers, which is a second-order geoelectric parameter (Maillet, 1947).

The total longitudinal conductance was computed using the expression:

$$\sum_{i=1}^n \frac{h_i}{\rho_i} \quad (3)$$

The overburden protective capacity of the study area was ascertained using the total longitudinal unit conductance values obtained in Equation (3) for each VES point (Henriet, 1976; Oladapo et al., 2004). The protective capacity of the area was evaluated using (Oladapo & Akintoriwa, 2007) rating (Table 1) which enables the classification of aquifer protective capacity into poor, weak, moderate, good, very good or excellent. Areas in the dumpsite rated poor, weak or moderate, are susceptible to contamination from leachate or other near surface pollution events.

For 2-D inversion, measured 2-D apparent resistivity data were analyzed and then correctly inverted to produce the 2-D resistivity-depth structure which aligned correctly with the actual subsurface resistivity and indicates the leachate plume. DIPPRO 2-D inversion program designed by “Korea Institute of Geoscience and Mineral Resources” (KIGAM, 2001) was employed, and small iterations set were

**Table 1.** Longitudinal conductance/protective capacity rating (After Oladapo & Akintoriwa, 2007).

Total longitudinal conductance (mhos)	Overburden protective capacity classification
	Aquifer vulnerability rating
<0.10	Poor
0.1 - 0.19	Weak
0.2 - 0.69	Moderate
0.7 - 4.9	Good
5 - 10	Very good
>10	Excellent

used while anticipating a good match between the 2-D inverted model of apparent resistivity along with the geological model indicating that the leachate contaminant has infiltrated the layer (Omolayo & Tope, 2014).

To conduct 3-D resistivity inversion, all the orthogonal 2-D data set (i.e. profiles LY<sub>1</sub> - LY<sub>6</sub> and LX<sub>1</sub> - LX<sub>6</sub>) were collated based on the RES2DINV collation code, and combined to form a 3-D data set that could be processed using a default 3-D inversion program (Ahzegbobor et al., 2010). The 3-D data set was inverted with RES3DINV program (Loke, 1994). RES3DINV program was utilized to invert the 3-D data to obtain horizontal depth slices in the *x-y* plane using numerical procedure based on the smoothness constrained least-squares technique (de Groot-Hedlin & Constable, 1990; Sasaki, 1992).

### 3. Results, Interpretation and Discussion

#### 3.1. Vertical Electrical Sounding (VES)

Interpretation of the VES data reveal 4 - 5 geo-electric layers within the subsurface. From the layer parameters (resistivity and thickness) and to constrain the interpretation, a threshold value was chosen for leachate contaminated layers as layers with relatively low resistivity values below 100 Ω·m ( $\rho < 100 \Omega\cdot m$ ) is indicative of the presence of electrically conductive leachate contaminant, which has a lower electrical resistivity compared to water. Therefore, the presence of leachate plumes in the soil/subsoil reduces soil's resistivity. Low resistivity anomalies indicative of leachate contamination were observed at various layers for VES 2, 3, 4, 5, 6, 7, 8, 9, and 10 (Table 2). In VES 2 within the second and third layers, low resistivity anomalies ( $\rho < 100 \Omega\cdot m$ ) were observed indicating leachate contamination within these layers, at depth of 3.2 m in the second layer and 9.1 m in the third layer (Table 2). In VES 3 within the second layer, low resistivity

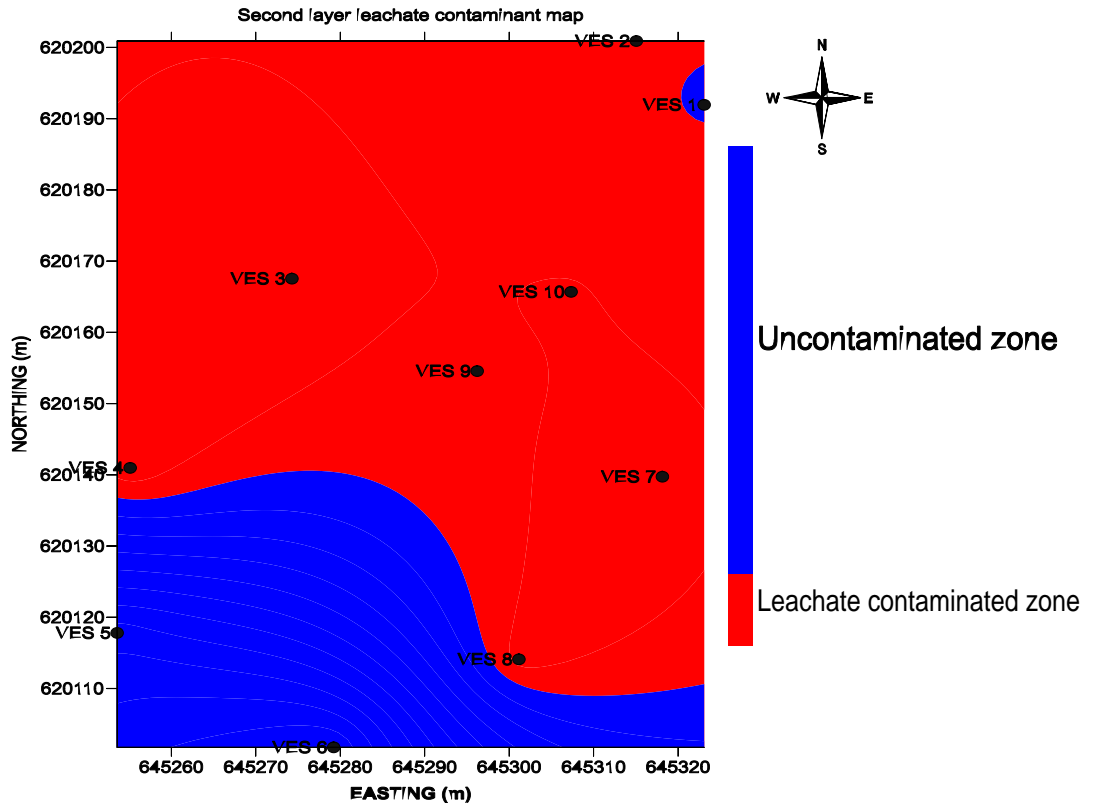
**Table 2.** Summary of VES 1-D model results, showing resistivity values, depth, thicknesses and leachate contaminated geo-electric layers.

VES No.	Layer resistivity ( $\rho_1/\rho_2/\rho_3/\dots/\rho_n$ )	Layer thickness ( $h_1/h_2/h_3/\dots/h_n$ )	Layer depth ( $d_1/d_2/d_3/\dots/d_n$ )	Inference
VES 1	1139.10/105.0/1082.2/101.0/2000.4/237.2	0.4/0.8/4.2/6.5/49.2/-	0.4/1.2/5.4/11.9/61.1/-	
VES 2	139.80/90.50*/68.1*/1547.9/7562.8	0.8/2.5/5.9/29.1/-	0.8/3.2/9.1/38.2/-	*Plume layer
VES 3	115.3/44.3*/183.6/568.0	0.8/5.0/12.6/-	0.8/5.8/18.4/-	*Plume layer
VES 4	104.20/13.20*/114.0/1215.0	0.6/2.5/10.9/-	0.6/3.1/14.0/-	*Plume layer
VES 5	334.40/477.0/78.50*/1290.0/117.40	0.6/1.3/7.2/22.5/-	0.6/1.9/9.1/31.5/-	*Plume layer
VES 6	499.80/650.70/179.80/59.10*/995.20	0.6/1.4/8.0/5.6/-	0.6/2.0/10.0/15.5/-	*Plume layer
VES 7	228.60/44.90*/865.50/113.90/2744.20	0.4/1.2/4.6/18.6/-	0.4/1.6/6.2/24.8/-	*Plume layer
VES 8	652.20/31.0*/94.40*/227.50	0.5/1.2/5.8/-	0.5/1.7/7.5/-	*Plume layer
VES 9	192.0/58.90*/389.50/2042.0/92.80*	0.7/5.9/9.9/25.4/-	0.7/6.5/16.4/41.8/-	*Plume layer
VES 10	172.50/47.80*/161.30/1866.10/159.60	0.9/3.6/9.5/44.9/-	0.9/4.5/14.0/58.9/-	*Plume layer

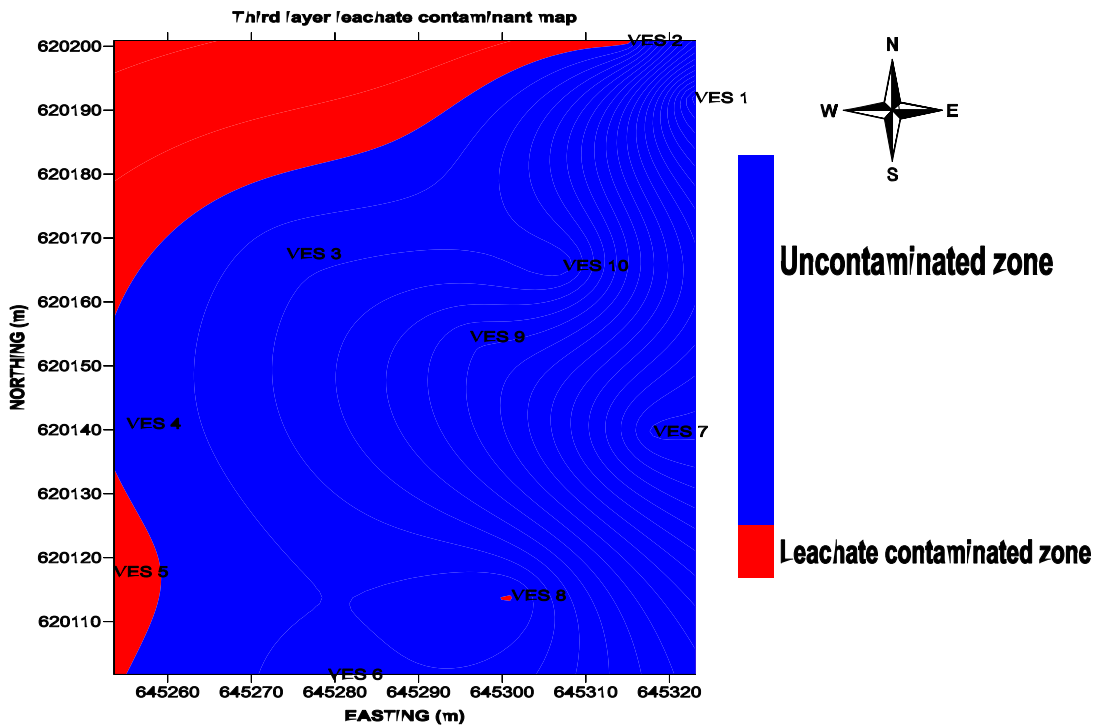
\*Leachate plume contaminated layer.

anomalies ( $\rho < 100 \Omega\cdot\text{m}$ ) was observed indicating leachate contamination within this layer, at depth of 5.8 m (**Table 2**). In VES 4, a low resistivity anomaly ( $\rho < 100 \Omega\cdot\text{m}$ ) was observed in the second layer indicating presence of leachate contamination within this layer at depth of 3.1 m (**Table 2**). In VES 5, leachate contamination was observed at the third layer at depth of 9.1 m, while in VES 6, leachate contamination was observed at the fourth layer at depth of 15.5 m (**Table 2**). In VES 7 within the second geo-electric layer, low resistivity anomaly ( $\rho < 100 \Omega\cdot\text{m}$ ) was observed indicating leachate contamination within this layer, at depth of 1.6 m (**Table 2**). In VES 8 within the second and third layers, low resistivity anomalies ( $\rho < 100 \Omega\cdot\text{m}$ ) were observed indicating leachate contamination within these layers, at depth of 1.7 m in the second layer and 7.5 m in the third layer (**Table 2**). In VES 9 within the second and fifth layers, low resistivity anomalies ( $\rho < 100 \Omega\cdot\text{m}$ ) were observed indicating leachate contamination within these layers, at depth of 6.5 m in the second layer and in the fifth layer at a depth beyond 41.8 m (depth to the overlying fourth layer), since the depth to the fifth layer could not be determined because current terminated in this zone (**Table 2**). In VES 10, leachate contamination was observed in the second layer at depth of 4.5 m (**Table 2**). There was no evidence of leachate contamination within the layers of VES 1 as observed from its 1-D resistivity models (**Table 2**). The 1-D resistivity model shows leachate contamination at the second layers for VES 2, 3, 4, 7, 8, 9, and 10 (**Table 2**) and third geo-electric layers for VES 2, 5 and 8 (**Table 2**) based on low resistivity values. Leachate contaminant maps of second and third layers estimated using the inverted resistivity values for VES 1 - 10 (**Figure 6(a)** & **Figure 6(b)**) reveals the extent of contamination due to leachate pollution ( $\rho < 100 \Omega\cdot\text{m}$ ) and the uncontaminated zone ( $\rho > 100 \Omega\cdot\text{m}$ ) within these layers. The contaminant maps (**Figure 6(a)** & **Figure 6(b)**) show that leachate pollution in the study area was more predominant within the second geo-electric layers (**Figure 6(a)**) than observed in the third layers (**Figure 6(b)**). Leachate contaminant depth contour map estimated for the second layers for VES 2, 3, 4, 7, 8, 9, and 10 is shown in **Figure 7(a)**. The map shows that the second layer has been completely invaded by leachate pollution from the surface up to a depth of 6.5 m, based on the low resistivity model values observed, with VES 9 having the deepest contamination depth of 6.5 m (**Table 2**). This indicates that within the second layer, the flow of leachate contamination is towards VES 9 (as indicated). **Figure 7(b)** shows the direction of groundwater flow in the study area. Groundwater flows from areas with high hydraulic gradients to areas with low hydraulic gradients. Therefore, the groundwater movement in the dumpsite is towards the northeastern (N-E) part of the dumpsite (as indicated), which is in agreement with the flow direction reported in *Ofomola et al., (2016)*.

**Table 3** summarizes the results of longitudinal conductance of the overburden aquifer unit in the study area calculated for VES 1 - 10. The longitudinal conductance values in **Table 3** were used to create a protective capacity map using terrain and 3-D surface modeling software (*Surfer, 2002*), using the advanced contour level option. In **Figure 8**, the longitudinal conductance map shows that



(a)



(b)

**Figure 6.** (a) Second layer contaminant map used to image leachate contaminated and uncontaminated locations within this layer for VES 1 – 10; (b) Third layer contaminant map used to image leachate contaminated and uncontaminated locations within this layer for VES 1 - 10.

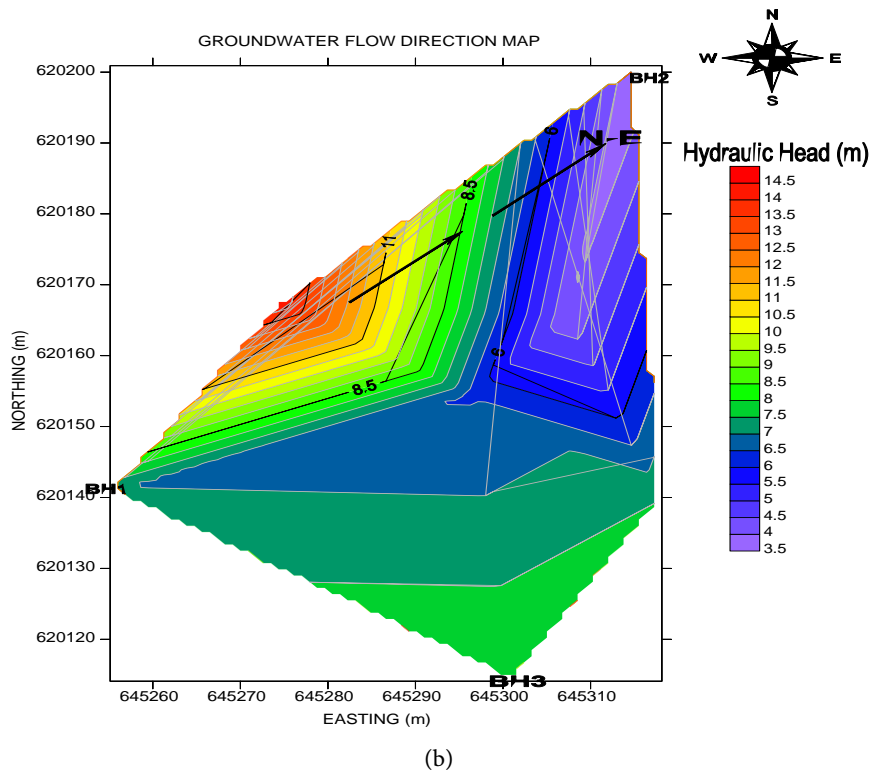
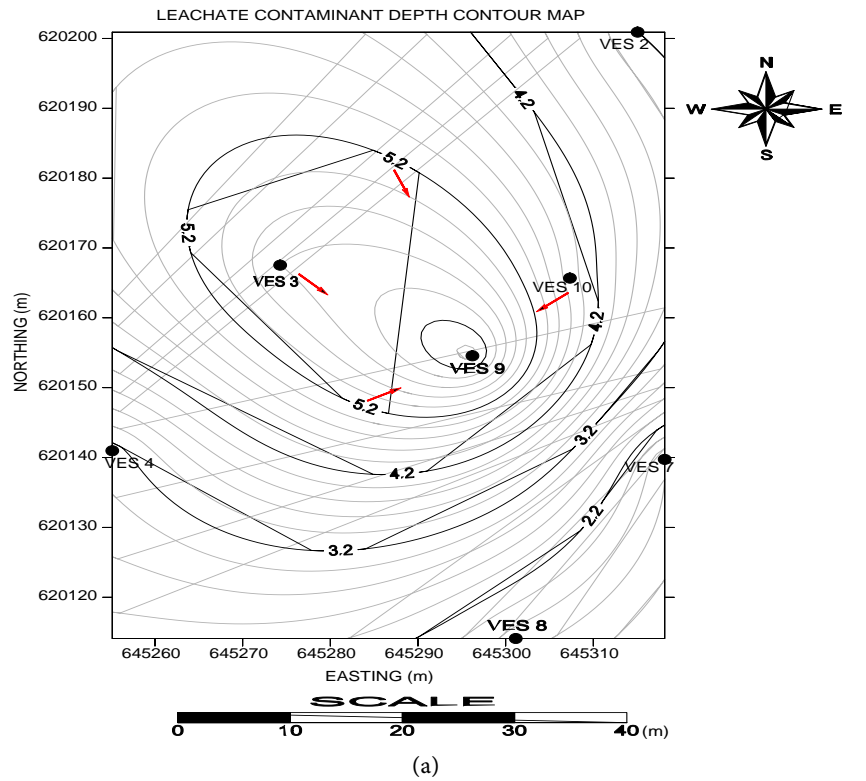


**Figure 7.** (a) Leachate contaminant depth-contour map of second layer showing depth to contaminated layers from surface for VES 2, 3, 4, 7, 8, 9, and 10. The map reveal that the second layers in VES 2, 3, 4, 7, 8, 9, and 10 have been completely invaded by leachate pollution up to depth of 6.5 m in the subsurface; (b) Calibrated hydraulic head distribution showing the groundwater flow in the dumpsite (arrows indicate the flow direction).

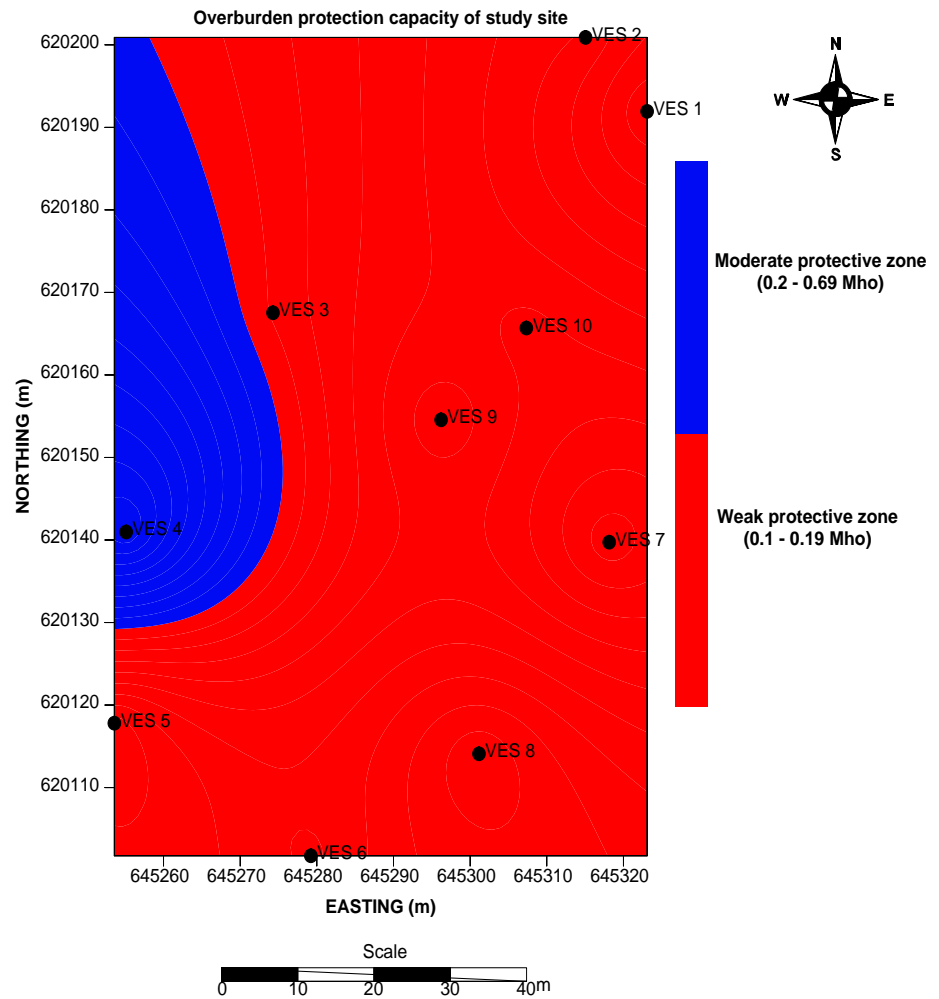


**Figure 8.** Longitudinal conductance map of VES locations 1 - 10 in the dumpsite, showing the overburden protective capacity.

**Table 3.** Summary of result of longitudinal conductance of overburden aquifer unit computed from geo-electric data.

VES Stn.	Layer resistivity ( $\rho_1/\rho_2/\rho_3/.../\rho_n$ )	Layer thickness ( $h_1/h_2/h_3/.../h_n$ )	$\sum_{i=1}^n \frac{h_i}{\rho_i}$	Aquifer protective capacity
VES 1	1139.10/105.0/1082.2/101.0/2000.4	0.4/0.8/4.2/6.5/49.2	0.1008	Weak*
VES 2	139.80/90.50/68.1/1547.9	0.8/2.5/5.9/29.1	0.13877	Weak*
VES 3	115.3/44.3/183.6	0.8/5.0/12.6	0.18844	Weak*
VES 4	104.20/13.20/114.0	0.6/2.5/10.9	0.29076	Moderate**
VES 5	334.40/477.0/78.50/1290.0	0.6/1.3/7.2/22.5	0.11371	Weak*
VES 6	499.80/650.70/179.80/59.10	0.6/1.4/8.0/5.6	0.14259	Weak*
VES 7	228.60/44.90/865.50/113.90	0.4/1.2/4.6/18.6	0.19708	Weak*
VES 8	652.20/31.0/94.40	0.5/1.2/5.8	0.10092	Weak*
VES 9	192.0/58.90/389.50/2042.0	0.7/5.9/9.9/25.4	0.14168	Weak*
VES 10	172.50/47.80/161.30/1866.10	0.9/3.6/9.5/44.9	0.16348	Weak*

\*Weak protective capacity (0.1 - 0.19 Mho); \*\*Moderate protective capacity (0.2 - 0.69 Mho).

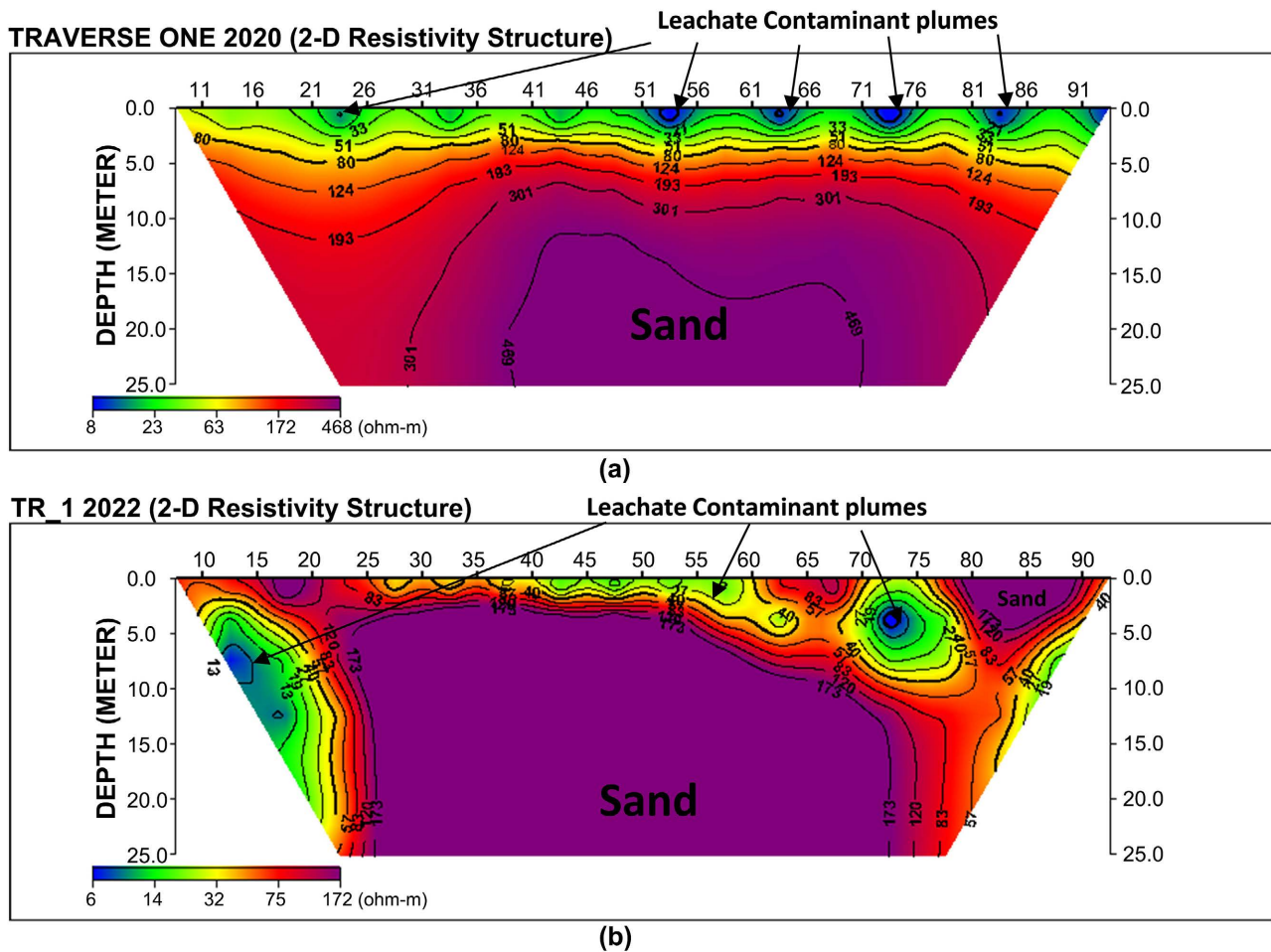
almost the entire area in the dumpsite is unprotected. Apart from VES 4 location which is moderately protected (0.2 - 0.69 Mho) (**Figure 8**), the remaining VES locations VES 1, 2, 3, 5, 6, 7, 8, 9 and 10 have weak protective capacities (0.1 - 0.19 Mho), and are susceptible to aquifer contamination due to leachate pollution from the dumpsite.

These findings show that the first aquifer (about 4.5 - 6.0 m) accessed through shallow wells is completely invaded by leachate pollution up to depth of 6.5 m, while the second aquifer (about 7.6 - 9.5 m) and third aquifer accessed through boreholes may be vulnerable to pollution due to weak protection capacity predominant of the VES locations in the dumpsite (**Figure 8**).

### 3.2. 2-D Electrical Resistivity Tomography (ERT)

The results of 2-D ERT for five (5) traverses ( $Ly_1$ ,  $Lx_1$ ,  $Lx_4$ ,  $Ly_5$  and  $Ly_6$ ) and three (3) recently acquired 2-D traverses in time-lapse mode (TR\_1, TR\_2 and TR\_3) as shown on the base map (**Figure 5**) was presented as 2-D resistivity-depth sections. The 2-D traverse TR\_1 was acquired along traverse 1 labeled as  $Ly_6$  on the base map (**Figure 5**), 2-D traverse TR\_2 was acquired along traverse 2 labeled as  $Lx_1$  on the base map (**Figure 5**), while 2-D traverse TR\_3 was acquired along traverse 6 labeled as  $Lx_4$  on the base map (**Figure 5**). The 2-D resistivity section for traverse 1 ( $Ly_6$ ) revealed a low resistivity structure (between 8 to 23  $\Omega\cdot m$ ) at the near surface (<5 m) between electrode positions 20 - 28 m, 51 - 56 m, 61 - 68 m, 71 - 76 m, 81 - 86 m and 91 - 100 m (**Figure 9(a)**). This low resistivity anomaly is due to the presence of conductive leachate plumes from the dumpsite that are gradually infiltrating the subsurface. The 2-D resistivity section of traverse TR\_1 acquired in 2022 along traverse  $Ly_6$  revealed a very low resistivity anomaly (between 6 to 14  $\Omega\cdot m$ ) at depth of 5.0 - 20.0 m between electrode position 10 - 15 m, and at the near surface (0 - 5.0 m) between electrode position 70 - 75 m (**Figure 9(b)**). This low resistivity anomaly is due to the presence of leachate plume within the subsurface. It is suffice to note that the amplitude of resistivity anomaly of the leachate plume observed in traverse TR\_1 (**Figure 9(b)**) acquired in the dumpsite in January 2022 along traverse  $Ly_6$  was much lower (between 6 to 14  $\Omega\cdot m$ ) than the resistivity anomaly observed in traverse  $Ly_6$  acquired in 2020 (between 8 to 23  $\Omega\cdot m$ ) as shown in **Figure 9(a)**. This observation is caused by time-lapse attenuation effect on the resistivity of the observed leachate contaminants overtime. Attenuation here is caused by long-time degradation processes and redox reactions (Giang et al., 2018) that occurred in the dumpsite resulting in more conductive leachate. As conductivity is inversely related to resistivity (Equations (1) and (2)), a highly conductive leachate plume has a lower resistivity signature on the resistivity tool than the less conductive plume. These findings explain why the amplitude of the resistivity anomaly of leachate contaminant observed in traverse TR\_1 in 2022 is much lower than that observed in traverse  $Ly_6$  in 2020. This could result to an increase in soil corrosivity in the area, because the higher the conductivity, the more likely is to corrode, which may increase soil corrosiveness in the area (Oyinkanola et al., 2016).

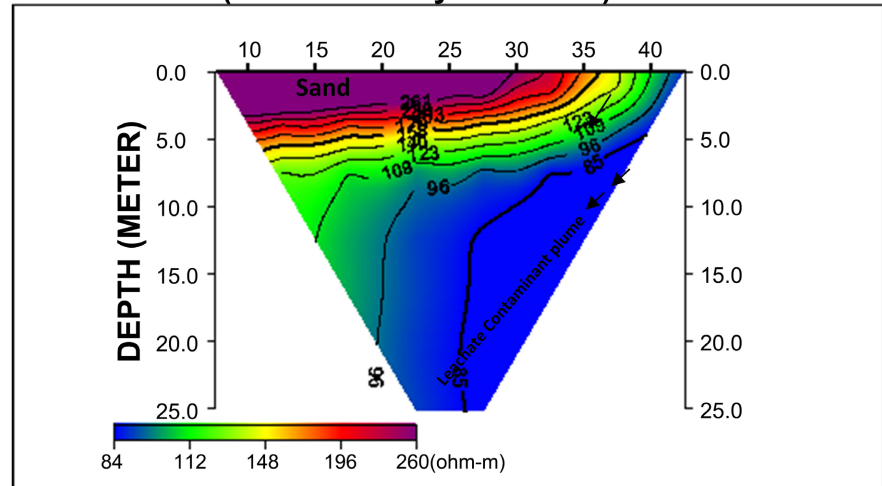




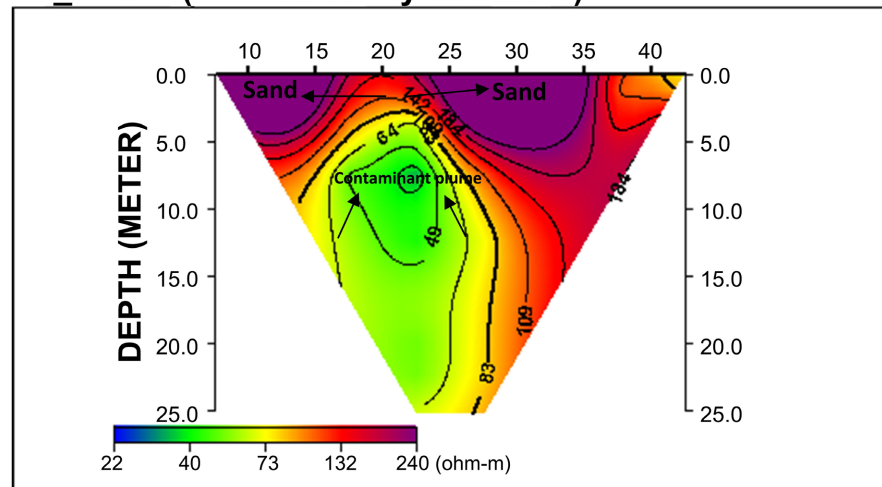
**Figure 9.** (a) 2-D resistivity-depth section of traverse 1 (LY<sub>6</sub>) in 2020; (b) 2-D resistivity-depth section of traverse TR\_1 acquired along LY<sub>6</sub> in 2022, showing the 2-D resistivity structure in the subsurface.

The 2-D resistivity section of traverse 2 (Lx<sub>1</sub>) revealed a low resistivity structure with resistivity (between 84 to 90 Ω·m) at electrode position of 38 - 50 m (Figure 10(a)). This low resistivity structure shows leachate contaminants from the dumpsite that infiltrates downward to depth beyond 15 m within the subsurface (Figure 10(a)). The 2-D resistivity section for traverse TR\_2 acquired along traverse Lx<sub>1</sub> in January 2022 (Figure 10(b)) revealed a low resistivity anticlinal structure (between 22 to 40 Ω·m) at a depth of 5.0 - 25.0 m which is indicative of leachate plume within the subsurface. This low resistivity anticlinal structure is sandwiched between two high resistivity structures ( $\rho \geq 240 \Omega \cdot m$ ) at the near surface (<5 m) indicating sand. Again, time-lapse attenuation effect was observed in the resistivity anomaly of leachate contaminant in traverse TR\_2 acquired in January 2022 shown in Figure 10(b) compared to the resistivity anomaly of leachate plume observed in traverse Lx<sub>1</sub> acquired in 2020 (Figure 10(a)).

The 2-D resistivity section of traverse 6 (Lx<sub>4</sub>) revealed a low resistivity structure (between 75 to 90 Ω·m) at depth of 0 - 5 m at electrode position 0 - 25 m

**TRAVERSE 2 (2-D Resistivity Structure)**

(a)

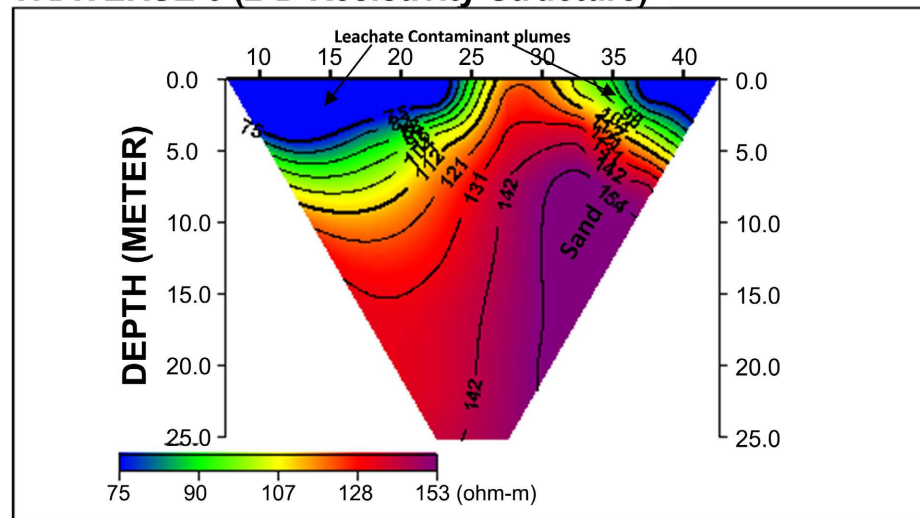
**TR\_2 2022 (2-D Resistivity Structure)**

(b)

**Figure 10.** (a) 2-D resistivity-depth section of traverse 2 ( $Lx_1$ ) in 2020; (b) 2-D resistivity-depth section of traverse TR\_2 acquired along  $Lx_1$  in 2022, showing the 2-D resistivity structure in the subsurface.

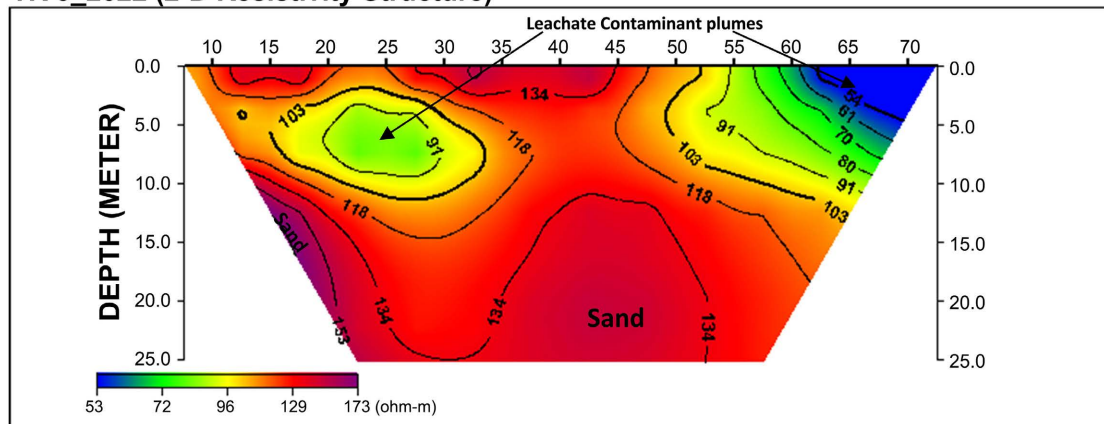
and at the near surface (<5 m) at electrode position 35 - 50 m (**Figure 11(a)**). These low resistivity structures indicate leachate contaminants from the dumpsite. The 2-D resistivity section of traverse TR\_3 acquired along traverse  $Lx_4$  in January 2022 (**Figure 11(b)**) has a low resistivity structure (between 53 to 72  $\Omega \cdot m$ ) at depth of 5.0 - 10.0 m at electrode position 20 - 30 m and at depth of 0 - 10 m at electrode position 55 - 80 m which are indicative of leachate contaminant plumes within the subsurface. Again, time-lapse attenuation was observed on the amplitude of the leachate resistivity observed in traverse  $Lx_4$  acquired in 2020 and traverse TR\_3 acquired in January 2022 (**Figure 11(a)** & **Figure 11(b)**). In traverse TR\_3 (**Figure 11(b)**) the leachate resistivity (between 53 to 72  $\Omega \cdot m$ ) is lower than the leachate resistivity (between 75 to 90  $\Omega \cdot m$ ) observed in traverse

### TRAVERSE 6 (2-D Resistivity Structure)



(a)

### TR 3\_2022 (2-D Resistivity Structure)

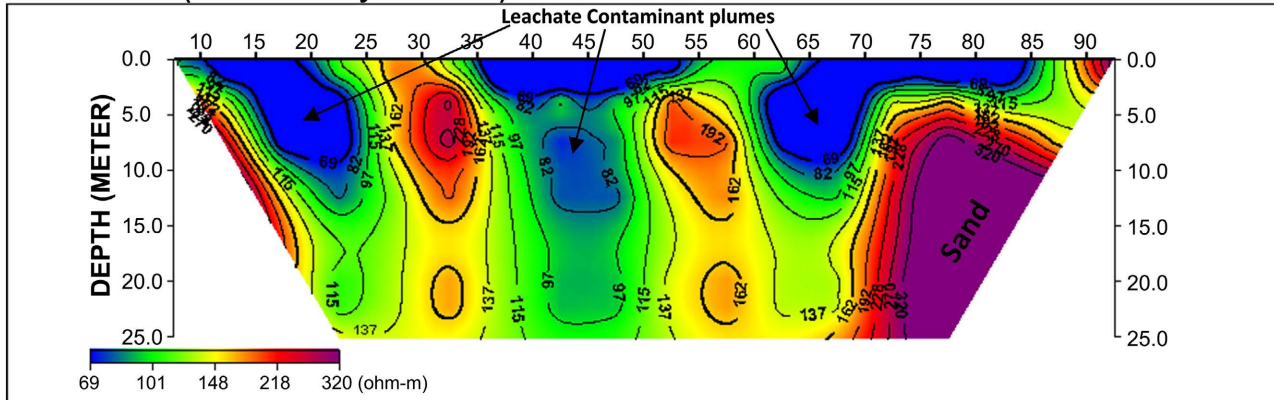


(b)

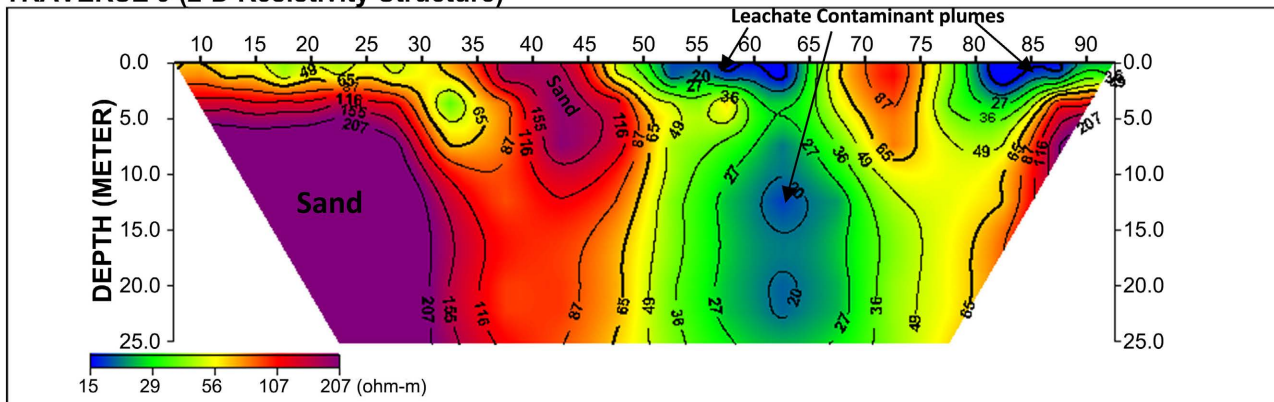
**Figure 11.** (a) 2-D resistivity-depth section of traverse 6 ( $Lx_4$ ) in 2020; (b) 2-D resistivity-depth section of traverse TR\_3\_2022 acquired along  $Lx_4$  in 2022, showing the 2-D resistivity structure in the subsurface.

$Lx_4$  acquired in 2020 (Figure 11(a)). The 2-D resistivity section for traverse 3 ( $Ly_1$ ) shown in Figure 12, revealed low resistivity structures (between 69 to 85  $\Omega \cdot m$ ) at electrode positions 0 - 20 m, 35 - 55 m and 65 - 95 m at depth of 0 - 10.0 m, 0 - 20.0 m and 0 - 15 m respectively. This is caused by the presence of leachate plumes infiltrating the subsurface. 2-D resistivity section for traverse 9 ( $Ly_5$ ) shown in Figure 13, revealed low resistivity (15 to 29  $\Omega \cdot m$ ) leachate plume at electrode positions 50 - 65 m and 80 - 100 m at depth beyond 25.0 m from the surface and at a depth of 10.0 m respectively.

The result of 2-D resistivity imaging shows the prevalence of low resistivity leachate plumes which have infiltrated into the subsurface within the depth imaged and have completely invaded groundwater sources and the underlying geology of the area thereby polluting the area and making its water unfit for consumption.

**TRAVERSE 3 (2-D Resistivity Structure)**

**Figure 12.** 2-D Resistivity tomography inversion section along traverse 3 ( $Ly_1$ ).

**TRAVERSE 9 (2-D Resistivity Structure)**

**Figure 13.** 2-D Resistivity tomography depth structure of traverse 9 ( $Ly_5$ ).

### 3.3. 3-D Electrical Resistivity Tomography (ERT)

The 3-D electrical resistivity tomography model obtained from inversion of the orthogonal set of 2-D apparent resistivity field data is shown in **Figure 14**. The 3-D model shows layers of leachate contaminant plume with low resistivity (13.8 - 56.9  $\Omega$ -m) from the dumpsite. The 3-D inversion model created after three iterative iteration routines yielded an 8.02% root mean square (RMS) error (**Figure 14**). The low RMS error obtained from the 3-D inversion is due to the good data points of the 3D grid simulated from the orthogonal series of 2-D traverses, and the 3-D resistivity model converges on the apparent resistivity data measured in the dumpsite. The subsurface resistivity model is valid, as the model represents a good compromise between the data fit and model smoothness in accordance with **Loke (2010)**. The depth slices revealed six layers at depths of 0.00 - 2.50 m in layer 1, 2.50 - 5.38 m in layer 2, 5.38 - 8.68 m in layer 3, 8.68 - 12.5 m in layer 4, 12.5 - 16.9 m in layer 5 and 16.9 - 21.9 m in layer 6 (see **Figure 14**). The Leachate plume was more pronounced in the first, second and third layers at depth ranging from 0.00 - 8.68 m. The 3-D inversion depth slices indicate that the contaminant plumes from the dumpsite are thought to have moved downward through the porous sandy layer to depth beyond 8.68 m.

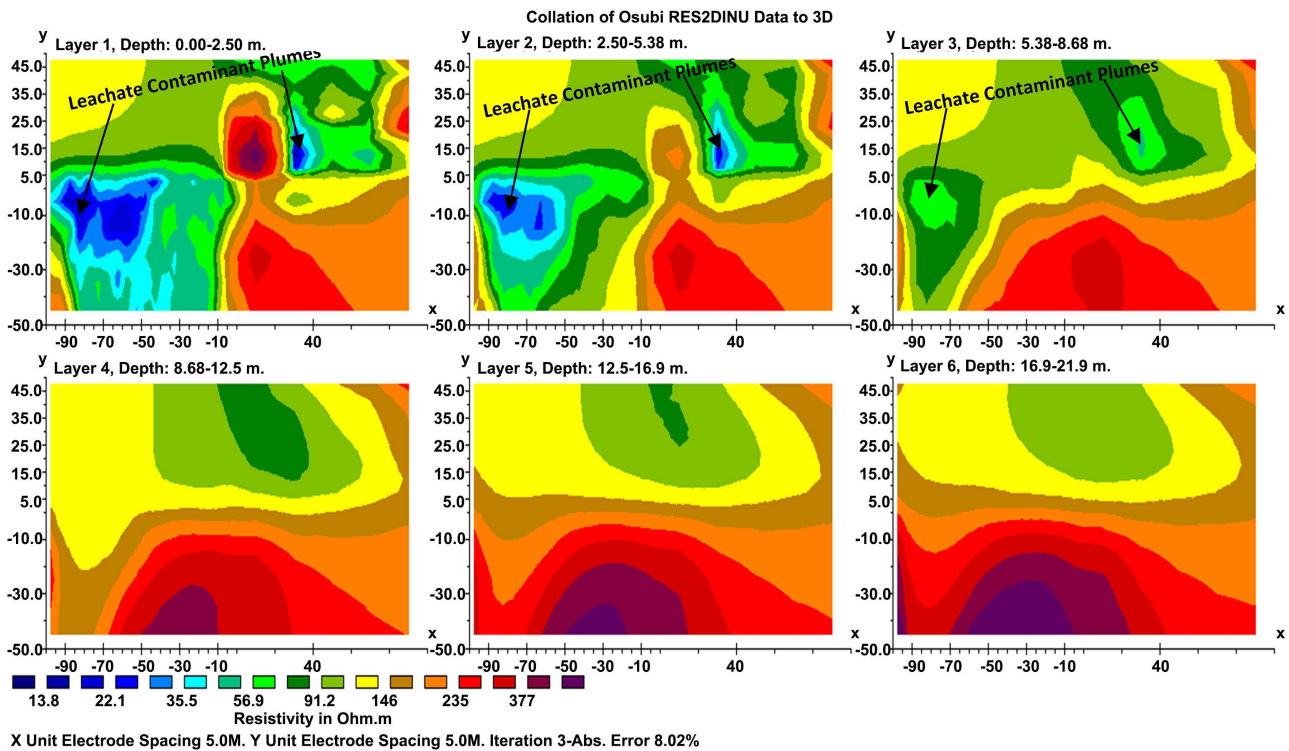


**Figure 14.** Six-layer horizontal depth slices simulated from 3-D resistivity inversion of the orthogonal 2-D traverses ( $L_y$  and  $L_x$  lines) using smoothness constrained least-squares inversion.

This depth exceeds the depth of water table in the area (between 4.5 - 6.0 m) and from the weak aquifer protective capacity (0.1 - 0.19 Mho) predominant in the area (Figure 8), it is obvious that groundwater pollution by leachate plume from the dumpsite cannot be avoided.

#### 4. Conclusion and Recommendation

Electrical resistivity is a near-surface non-invasive geophysical method that plays an important role in environmental assessment of pollution levels in soil, subsoil and groundwater source. An integrated geoelectrical method involving 3-D, 2-D, and 1-D techniques have been successfully employed in assessing the range of leachate contamination of an old dumpsite located in Osubi town, southern Nigeria. Our geophysical method was able to map and depict the lateral and vertical extents of the leachate plume from the dumpsite. 2D ERT data acquired in normal and time-lapse mode imaged a low resistivity leachate plume from the near surface (<5 m) to a depth of 25.0 m. Time-lapse 2D ERT data collected two years after normal data collection; show a leachate plume with lower resistivity anomaly which depicts attenuation of resistivity anomalies over time. 3D ERT imaged leachate contaminants within the first, second and third layers at depth ranging from 0.00 - 8.68 m within the subsurface, which improved the reliability level of resistivity imaging. Thus, leachate contamination clearly increased beyond the depth to the first and second aquifers of the area, and domestically available

groundwater was contaminated with leachate from the dumpsite. Longitudinal conductance map of the area shows that the areas' protective capacity is weak. As a result, the aquifers in this area are vulnerable to pollution from the dumpsite due to their weak protection capacity. The collation of orthogonal series of 2-D resistivity data into a 3-D dataset is a fast and effective data acquisition design for 3-D electrical resistivity measurement. The techniques used in this study (2-D, 3-D ERT and 1-D VES) justifiably provided relevant information regarding the degree of contamination caused by the landfill leachate plume. The benefits of integrating these geoelectrical techniques (3-D, 2-D, and 1-D) to depict contaminated areas of the environment and groundwater are its' cost effectiveness, rapidity of operation, suitability of the techniques for wider application in other areas of environmental pollution studies and a wider areal coverage unlike other techniques (borehole method and chemical analysis of soil and water) that provide limited spatial information. Therefore, it is highly recommended that these techniques be employed as an important geophysical tool for environmental assessment of contaminated sites.

In view of the results of this study, the following considerations are recommended:

- Environmental remediation and leachate management processes *i.e.* leachate recirculation, which collects leachate and re-injects it into the waste mass to accelerate its decomposition should be carried out in the dumpsite. This process converts the leachate volume into landfill gas, thereby reducing the total amount of leachate discarded.
- Until the leachate treatment process is complete, the local population must have access to an alternative water source for domestic use.
- Landfills approved for waste disposal should be designed with a liner with high tensile strength and flexibility to maintain integrity and impermeability throughout the life of the landfill. This isolates the leachate in the embankment from the surrounding environment, protects the underlying soil and groundwater and prevents future pollution.

## Acknowledgements

The authors profoundly acknowledge the management of Petroleum Training Institute (PTI) Effurun, Nigeria for allowing us carry out the geophysical survey at the dumpsite located close to the new PTI Osubi facility and to the Federal University of Petroleum Resources, Effurun, Nigeria for the use of her computing facilities.

## Availability of Data and Material

Applicable and available on demand from the corresponding author.

## Code Availability (Software Used)

DIPPROWIN, RES2DINV, RES3DINV, SUFER-13 and WINRESIST Suite.

## Declarations

### Ethics Approval and Consent to Participate

All the ethical principles of research in field data acquisition, preparation, analysis and interpretation were implemented.

### Conflicts of Interest

We declare that this research work has never been submitted previously by anyone to any journal for peer review and publication, hence it is an original work. The authors declare no competing interests.

## References

- Abdullahi, N. K., Osazuwa, I. B., & Sule, P. O. (2011). Application of Integrated Geophysical Techniques in the Investigation of Groundwater Contamination. A Case Study of Municipal Solid Waste Leachate. *Ozean Journal of Applied Science*, 4, 7-25.
- AGI [Advanced Geosciences, Inc.] (2003). *Earth Imager 2-D Resistivity Inversion Software, Version 1.5.10*. Advanced Geosciences, Inc.
- Ahzegebor, A. P., Olayinka, A. I., & Singh, V. S. (2010). Application of 2D and 3D Geoelectrical Resistivity Imaging for Engineering Site Investigation in a Crystalline Basement Terrain, Southwestern Nigeria. *Environmental Earth Science*, 61, 1481-1492. <https://doi.org/10.1007/s12665-010-0464-z>
- Akpoborie, I. A., Etobro, A. A. I., Nfor, B., & Odagwe, S. (2011). Aspects of the Geology and Groundwater Conditions of Asaba, Nigeria. *Archives of Applied Science Research*, 3, 537-550.
- Akpokodje, E. G., & Etu-Efeotor, J. O. (1987) The Occurrence and Economic Potential of Clean Sand Deposits of the Niger Delta. *Journal of African Earth Sciences*, 6, 61-65. [https://doi.org/10.1016/0899-5362\(87\)90107-2](https://doi.org/10.1016/0899-5362(87)90107-2)
- Akuijeze, C. N., & Ohaji, S. M. O. (1989). *Iron in Borehole water in Bendel State*. Nigeria Association of Hydrogeologists.
- Aseez, O. L. (1989). *Review of the Stratigraphy, Sedimentation and Structure of the Niger Delta*. In C. A. Kogbe (Ed.), *Geology of Nigeria* (pp. 311-324). Rockview Nigeria Limited.
- Ayolabi, E. A., Adetayo, F. F., & Olusola, T. K. (2013). Integrated Geophysical and Geochemical Methods for Environmental assessment of Municipal Dumpsite System. *International Journal of Geosciences*, 4, 850-862. <https://doi.org/10.4236/ijg.2013.45079>
- Bernstone, C., & Dahlin, T. (1999). Assessment of Two Automated DC Resistivity Data Acquisition Systems to Landfill Location Surveys. Two Case Studies. *Journal of Environmental and Engineering Geophysics*, 4, 113-121. <https://doi.org/10.4133/JEEG4.2.113>
- Bjerg, P. L., Albrechtsen, H. J., Kjeldsen, P., Christensen, T. H., & Cozzarelli, I. M. (2014). The Biogeochemistry of Contaminant Groundwater Plumes Arising from Waste Disposal Facilities. In H. D. Holland, & K. K. Turekian (Eds.), *Treatise on Geochemistry* (2nd ed., Vol. 11, pp. 573-605). Elsevier. <https://doi.org/10.1016/B978-0-08-095975-7.00916-5>
- Bjerg, P. L., Ruge, K., Cortsen, J., Nielsen, P. H., & Christensen, T. H. (1999). Degradation of Aromatic and Chlorinated Aliphatic Hydrocarbons in the Anaerobic Part of the Grindsted Landfill Leachate Plume: *In Situ* Microcosm and Laboratory Batch Experiments. *Groundwater*, 37, 113-121. <https://doi.org/10.1111/j.1745-6584.1999.tb00964.x>

- Carpenter, P. J., Kaufmann, R. S., & Price, B. (2012). Use of Resistivity Soundings to Determine Landfill Structure. *Ground Water*, 28, 569-575. <https://doi.org/10.1111/j.1745-6584.1990.tb01713.x>
- Christensen, T. H., Kjeldsen, P., Bjerg, P. L., Jensen, D. L., Christensen, J. B., Baun, A., Albrechtsen, H.-J., & Heron, G. (2001). Biogeochemistry of Landfill Leachate Plumes. *Applied Geochemistry*, 16, 659-718. [https://doi.org/10.1016/S0883-2927\(00\)00082-2](https://doi.org/10.1016/S0883-2927(00)00082-2)
- Chung, S., Zheng, J., Burket, S., & Brooks, B. (2018). Select Antibiotics in Leachate from Closed and Active Landfills Exceed Thresholds for Antibiotic Resistance Development. *Environment International*, 115, 89-96. <https://doi.org/10.1016/j.envint.2018.03.014>
- Cozzarelli, I. M., Boehlke, J. K., Masoner, J., Breit, G. N., Lorah, M. M., Tuttle, M. L. W., & Jaeschke, J. B. (2011). Biogeochemical Evolution of a Landfill Leachate Plume, Norman, Oklahoma. *Ground Water*, 49, 663-687. <https://doi.org/10.1111/j.1745-6584.2010.00792.x>
- Cristina, P., Cristina, D., Alicia, F., & Pamela, B. (2012). Application of Geophysical Methods to Waste Disposal Studies. In X.-Y. Yu (Ed.), *Municipal and Industrial Waste Disposal* (pp. 1-5). IntechOpen. <https://doi.org/10.5772/29615>
- de Groot-Hedlin, C., & Constable, S. C. (1990). Occam's Inversion to Generate Smooth Two-Dimensional Models from Magnetotelluric Data. *Geophysics*, 55, 1613-1624. <https://doi.org/10.1190/1.1442813>
- Doust, H., & Omatsola, E. (1990). Niger-Delta. In J. D. Edwards, & P. A. Santogrossi (Eds.), *Divergent/Passive Margin Basins* (AAPG Memoir No. 48, pp. 239-248). American Association of Petroleum Geologists. <https://doi.org/10.1306/M48508C4>
- Ganiyu, S. A., Badmus, B. S., Oladunjoye, M. A., Aizebeokhai, A. P., & Olurin, O. T. (2015). Delineation of Leachate Plume Migration Using Electrical Resistivity Imaging on Lapite Dumpsite in Ibadan, Southwestern Nigeria. *Geosciences*, 5, 70-80.
- Giang, N. V., Kochanek, K., Vu, N. T., & Duan, N. B. (2018). Landfill Leachate Assessment by Hydrological and Geophysical Data: Case Study NamSon, Hanoi, Vietnam. *Journal of Material Cycles and Waste Management*, 20, 1648-1662. <https://doi.org/10.1007/s10163-018-0732-7>
- Goes, B. J. M. & Meekes, J. A. C. (2004). An Effective Electrode Configuration for the Detection of DNAPLs with Electrical Resistivity Tomography. *Journal of Environmental and Engineering Geophysics*, 9, 127-141. <https://doi.org/10.4133/JEEG9.3.127>
- Henriet, J. P. (1976). Direct Application of the Dar-Zarrouk Parameters in Groundwater Surveys. *Geophysical Prospecting*, 24, 344-353. <https://doi.org/10.1111/j.1365-2478.1976.tb00931.x>
- Jegade, S. I., Ujuanbi, O., Abdullahi, N. K., & Iserhien-Ewekeme, R. E. (2012). Mapping and Monitoring of Leachate Plume Migration at an Open Waste Disposal Site Using Non-Invasive Methods. *Research Journal of Environmental and Earth Sciences*, 4, 26-33.
- Jhamnani, B., & Singh, S. K. (2009). Groundwater Contamination Due to Bhalaswa Landfill Site in New Delhi. *International Journal of Environmental Science and Engineering*, 1, 121-125.
- Kah, M., & Brown, C. D. (2007). Change in Pesticides Adsorption with Time at High Soil to Solution Ratio. *Chemosphere*, 68, 1335-1343. <https://doi.org/10.1016/j.chemosphere.2007.01.024>
- KIGAM [Korea Institute of Geoscience and Mineral Resources] (2001). *DIPRO Version 4.01, Processing and Interpretation Software for Electrical Resistivity Data*. Korea Institute of Geoscience and Mineral Resources.
- Kjeldsen, P., & Christophersen, M. (2001). Composition of Leachate from Old Landfills in



- Denmark. *Waste Management & Research*, 19, 249-256.  
<https://doi.org/10.1177/0734242X0101900306>
- Kulke, H. (1995). Nigeria. In H. Kulke (Ed.), *Regional Petroleum Geology of the World, Part II, Africa, America, Australia and Antarctica* (pp. 143-172). Gebruder Borntraeger.
- Lapworth, D. J., Baran, N., Stuart, M. E., & Ward, R. S. (2012) Emerging Organic Contaminants in Groundwater: A Review of Sources, Fate and Occurrence. *Environmental Pollution*, 163, 287-303. <https://doi.org/10.1016/j.envpol.2011.12.034>
- Loke, M. H. (1994). *The Inversion of Two-Dimensional Resistivity Data*. Unpublished PhD Thesis, University of Birmingham.
- Loke, M. H. (2000). *Electrical Imaging Surveys for Environmental and Engineering Studies: A Practical Guide to 2D and 3D Surveys* (p. 59).
- Loke, M. H. (2001). *Electrical Imaging Surveys for Environmental and Engineering Studies: A Practical Guide to 2D and 3D Surveys* (62 p).  
<http://www.geoelectrical.com/downloads.php>
- Loke, M. H. (2010). *Tutorial: 2-D and 3-D Electrical Imaging Surveys* (p. 95).  
<http://www.geoelectrical.com/downloads.php>
- Lyngkilde, J., & Christensen, T. H. (1992). Fate of Organic Contaminants in the Redox Zones of a Landfill Leachate Pollution Plume (Vejen, Denmark). *Journal of Contaminant Hydrology*, 10, 291-307. [https://doi.org/10.1016/0169-7722\(92\)90012-4](https://doi.org/10.1016/0169-7722(92)90012-4)
- Maillet, R. (1947). The Fundamental Equations of Electrical Prospecting. *Geophysics*, 12, 527-556. <https://doi.org/10.1190/1.1437342>
- Marylyn, V. Y. (1990). Modeling Microbial Transport in Soil and Groundwater. *Environmentalist*, 56, 324-327.
- Meju, M. A. (2000). Geoelectrical Investigation of Old/Abandoned, Covered Landfill Sites in Urban Areas: Model Development with a Genetic Diagnosis Approach. *Journal of Applied Geophysics*, 44, 115-150. [https://doi.org/10.1016/S0926-9851\(00\)00011-2](https://doi.org/10.1016/S0926-9851(00)00011-2)
- Merki, P. J. (1970). Structural Geology of the Cenozoic Niger Delta (pp. 251-268). University of Ibadan Press.
- Ofomola, M. O. (2015). Integrated Geophysical and Hydrogeochemical Studies of Shallow Aquifer Contamination in Osubi, Near Warri, Southern Nigeria. *Journal of Earth Sciences and Geotechnical Engineering*, 5, 79-102.
- Ofomola, M. O., Ako, B. D., & Adelusi, A. O. (2016). Flow Direction and Velocity Determination of Dumpsite-Induced Groundwater Contamination in Part of Delta State, Nigeria. *Arabian Journal of Geosciences*, 9, Article No. 398.  
<https://doi.org/10.1007/s12517-016-2405-y>
- Oladapo, M. I., & Akintorinwa, O. J. (2007). Hydrogeophysical Study of Ogbese, Southwestern, Nigeria. *Global Journal of Pure and Applied Sciences*, 13, 55-61.  
<https://doi.org/10.4314/gipas.v13i1.16669>
- Oladapo, M. I., Mohammed, M. Z., Adeoye, O. O., & Adetola, B. A. (2004). Geoelectrical in Vestigation of the Ondo State Housing Corporation Estate, Ijapo Akure, Southwestern Nigeria. *Journal of Mining and Geology*, 40, 41-48.  
<https://doi.org/10.4314/jmg.v40i1.18807>
- Olobaniyi, S. B., & Owoyemi, F. B. (2006). Characterization by Factor Analysis of the Chemical Facies of Groundwater in the Deltaic Plain Sands Aquifer of Warri, Western Niger Delta, Nigeria. *African Journal of Science and Technology*, 7, 73-81.  
<https://doi.org/10.4314/ajst.v7i1.55201>
- Omolayo, D., & Tope, F. J. (2014). 2D Electrical Imaging Surveys for Leachate Plume Migration at an Old Dumpsite in Ibadan South Western Nigeria: A Case Study. *Internation-*

- tional Journal of Geophysics*, 2014, Article ID: 879530.  
<https://doi.org/10.1155/2014/879530>
- Oyinkanola, L. O. A., Fajemiroye, J. A., Tijani, B. O., & Oke, D. A. (2016). Correlation between Soil Electrical Resistivity and Metal Corrosion Based on Soil Types for Structural Designs. *Scientific Research Journal (SCIRJ)*, 1, 26-29.
- Reyment, R. A. (1965). *Aspects of the Geology of Nigeria* (p. 132). University of Ibadan Press.
- Sasaki, Y. (1992). Resolution of Resistivity Tomography Inferred from Numerical Simulation. *Geophysical Prospecting*, 40, 453-464.  
<https://doi.org/10.1111/j.1365-2478.1992.tb00536.x>
- Short, K. C., & Stauble, A. J. (1967). Outline of the Geology of Niger Delta. *American Association of Petroleum Geologists Bulletin*, 51, 761-779.  
<https://doi.org/10.1306/5D25C0CF-16C1-11D7-8645000102C1865D>
- Surfer (2002). *Contouring and 3D Surface Mapping for Scientists and Engineers*. Golden Software Incorporation.
- Uchegbulam, O., & Ayolabi, E. A. (2014). Application of Electrical Resistivity Imaging in Investigating Groundwater Pollution in Sapele Area, Nigeria. *Journal of Water Resource and Protection*, 6, 1369-1379. <https://doi.org/10.4236/jwarp.2014.614126>
- Vander Velpen, B. P. A. (2004). *WinRESIST Version 1.0. Resistivity Sounding Interpretation Software*. M. Sc. Research Project, ITC Limited.
- Wigwe, G. A. (1975). The Niger Delta: Physical. In G. E. K. Ofomata (Ed.), *Nigeria in maps: Eastern States* (pp. 380-400). Ethiope Publishing House.
- Zonge, K., Wynn, J., & Urquhart, S. (2005). 9. Resistivity, Induced Polarization and Complex Resistivity. In: D. K. Butler (Ed.), *Near Surface Geophysics* (pp. 265-300). Society of Exploration Geophysics. <https://doi.org/10.1190/1.9781560801719.ch9>